ACS ES&T Air

pubs.acs.org/estair

Article

O_3 Sensitivity to NO_x and VOC During RECAP-CA: Implication for Emissions Control Strategies

Shenglun Wu, Christopher P. Alaimo, Yusheng Zhao, Peter G. Green, Thomas M. Young, Shang Liu, Toshihiro Kuwayama, Matthew M. Coggon, Chelsea E. Stockwell, Lu Xu, Carsten Warneke, Jessica B. Gilman, Michael A. Robinson, Patrick R. Veres, J. Andrew Neuman, and Michael J. Kleeman*

Cite This: *ACS EST Air* 2024, 1, 536–546

Read Online

ACCESS | Metrics & More | Article Recommendations | Supporting Information

ABSTRACT: Lack of recent progress in reducing ground-level ozone (O_3) concentrations to comply with health-based standards in the South Coast Air Basin (SoCAB) has motivated a reanalysis of emission control strategies. Here we used two parallel transportable smog chamber systems to measure the sensitivity of O_3 to volatile organic compounds (VOCs) and nitrogen oxides (NO_x = NO + NO_2) in Pasadena and Redlands, California from July to October, 2021. The transportable smog chamber system measures the ambient O_3 sensitivity and the ambient O_3 chemical regime by comparing O_3 formation in a basecase chamber and a perturbed chamber. The monthly median observed O_3 sensitivity in Pasadena was stable in the VOC-limited regime, but showed a seasonal trend in Redlands, where median O_3 sensitivity was VOC-limited in July and October and transitioned towards the NO_x-limited regime in August and September. Day-specific O_3 sensitivity at both Pasadena and Redlands could be either NO_x-limited or VOC-limited on O_3-nonattainment days. Calculated O_3 isopleths for Pasadena and Redlands were constructed using a photochemical box model based on comprehensive measurements of NO_x and VOCs during the Re-Evaluating the Chemistry of Air Pollutants in California (RECAP-CA) campaign. Calculated O_3 isopleths were in good agreement with the chamber measurements. The calculations suggest that an additional ~40% NO_x reduction is needed for Pasadena and Redlands to move 95% of the days with O_3 concentrations above 70 ppb to the NO_x-limited regime where further NO_x reductions will result in lower O_3 concentrations.

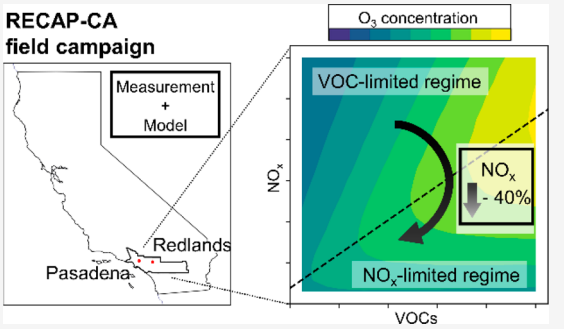

KEYWORDS: *ozone, volatile organic compounds, nitrogen oxides, O_3 sensitivity regime, control strategy*

1. INTRODUCTION

Ground-level ozone (O_3) forms in urban atmospheres from reactions of two main precursors: volatile organic compounds (VOCs = thousands of compounds containing carbon, hydrogen, and other elements) and nitrogen oxides (NO_x = NO + NO_2). The nonlinear response of O_3 formation to the initial concentration of VOCs and NO_x can be separated into two regimes: NO_x-limited and VOC-limited (also referred to as NO_x-saturated).[1] The NO_x-limited regime represents a low NO_x environment where the O_3 formation is limited by the photolysis of NO_2 or production of NO_2 from NO. Decreasing NO_x emissions in the NO_x-limited regime therefore reduces O_3 formation. The VOC-limited regime represents a high NO_x environment where NO_2 competes with VOCs for the hydroxyl radical ($^{\bullet}$OH) in a chain termination reaction to form nitric acid (HNO_3).[2] Decreasing NO_x emissions in the VOC-limited regime increases the O_3 concentrations, as less $^{\bullet}$OH is removed by NO_2. Effective O_3 control strategies account for the chemical regime and then target the anthropogenic sources that emit the limiting precursor.

Regulators in California's South Coast Air Basin (SoCAB) have been working to mitigate O_3 pollution for seven decades. The CalNex-2010 field campaign evaluated the impact of those efforts by comprehensively analyzing the precursors of O_3 formation in the SoCAB.[3] CalNex measurements suggested that the decreasing abundance of NO_x and VOC and the decreasing VOC/NO_x ratio in past decades greatly reduced the level of the O_3 concentrations.[4−6] Despite this past success, recent developments highlight the need to better understand present-day precursors of O_3 formation in the SoCAB. Between 2010 and 2020, the trend of decreasing O_3 concentrations slowed, and O_3 concentrations even increased in some locations within the SoCAB.[7,8] This behavior is consistent with a control strategy focused on NO_x emissions reductions in a VOC-limited atmosphere.[9−13] The observed increase in O_3 concentrations across multiple cities in response

Received: February 7, 2024
Revised: April 5, 2024
Accepted: April 5, 2024
Published: April 15, 2024

to short-term NO_x reductions during the COVID-19 lockdown[14−17] is consistent with this theory. Recent VOC measurements suggest that O_3 concentrations could be further reduced by controlling emissions of Volatile Chemical Products (VCPs),[18−20] but seasonal trends in the O_3 sensitivity regime suggest that biogenic VOC (BVOC) emissions may also significantly contribute to O_3 formation.[7] If uncontrollable biogenic VOCs produce significant O_3 concentrations, one approach that may be effective to reduce the O_3 concentration is a long-term NO_x reduction. It will be critically important to understand how much NO_x control is needed to reach the NO_x-limited regime if this strategy is implemented.[11,21] The traditional approach to analyzing O_3 sensitivity to NO_x and VOCs configures a box model[22,23] or chemical transport model[19,24] based on lab chamber measurements to reproduce the basecase observations from a field campaign. The traditional approach then trusts that the model calculation can accurately predict changes to ambient pollutant concentrations in response to emission perturbations with no ability to check the accuracy of those predictions.

Our past study[7] developed a transportable smog chamber system to directly measure the O_3 chemical regime in Sacramento, CA, by observing the O_3 response to NO_x and VOC perturbations. Long-term measurements in Sacramento identified a seasonal trend in O_3 sensitivity that moved from VOC-limited to NO_x-limited from spring to summer, and from NO_x-limited to VOC-limited from summer to winter. Here we extend those observations using two parallel systems to measure the sensitivity of the O_3 at two sites in the SoCAB during the Re-Evaluating the Chemistry of Air Pollutants in California (RECAP-CA) field campaign. Seasonal trends in the O_3 chemical regime are shown between July and October, 2021. The O_3 chemical regimes on days with recorded O_3 concentrations above 70 ppb are summarized. Utilizing the comprehensive VOC measurements during RECAP-CA, a chamber model is created with verified sensitivity of the O_3 to NO_x and VOCs to generate O_3 isopleth diagrams at both measurement sites to determine the amount of NO_x control needed to transition to NO_x-limited conditions.

2. METHODS

2.1. Field Measurement Descriptions. Measurements were taken at Pasadena and Redlands during the period July-October, 2021. The prevailing daytime winds transport pollution eastward (inland) in the surrounding region.[3] Pasadena represents a location near the urban core of Los Angeles, while Redlands represents an urban downwind area. The location of the sampling sites, meteorological trends, and wind direction are provided in Supporting Information (Figures S1−S4).

Measurements at Pasadena were taken on the campus of the California Institute of Technology (CIT) (34.140716, −118.122426). O_3, NO_x, NO_y (= NO_x + HNO_3 + acylperoxy nitrates + $ClNO_2$ + N_2O_5), and O_3 sensitivity were measured at CIT during July 16 to October 31, 2021. Additional measurements, including speciated VOC measurements, were made at the same site from August 7 to September 6, 2021 as part of the RECAP-CA field campaign. Nearby emissions sources include a university parking lot, power plant, cafeteria plus other facilities, and the residential/commercial sources in the surrounding city of Pasadena. A major freeway is located ∼1.2 km north of the Pasadena measurement site.

Measurements in Redlands were taken at the Dearborn Reservoir monitoring site maintained by the South Coast Air Quality Management District (SCAQMD) in Redlands, CA (34.059671, −117.147304). O_3, NO_x, NO_y, VOCs, and O_3 sensitivity were measured in Redlands during July 10 to October 31, 2021. Emissions sources close to the Redlands site include residential neighborhoods, a mixture of commercial and industrial land uses, and a university. A major freeway is located ∼1.5 km southwest of the Redlands sampling site.

2.2. Chamber Measurements. Two transportable smog chamber systems with similar configurations were used to measure the sensitivity of O_3 to NO_x and VOC perturbations in ambient air between 10 AM and 12 PM PDT once a day at each study site. The detailed configuration, operation, and performance of transportable smog chamber systems have been presented previously[7] and only a summary of the dual configuration and operation is presented here.

Both mobile chamber systems were configured with three identical 1 m^3 fluorinated ethylene propylene (FEP) smog chambers. One chamber was not perturbed; one chamber was perturbed by adding NO_x, and one chamber was perturbed by adding VOC. UV lamps above and below the chambers irradiated the trapped atmosphere with UV intensity similar to mid-day conditions in California during the summer (50 $W \cdot m^{-2}$).[25] Incoming chamber air was not filtered and therefore contained all gas- and particle-phase species in the ambient atmosphere. All chambers were drained after each test, then filled with clean air, and irradiated by UV lamps as a cleaning step prior to the next experiment. The cleaning cycle was repeated three times to mitigate possible carryover effects between experiments.

In the current study, all three smog chambers within each mobile system were filled with ambient air between 10 AM to 12 PM on each measurement day. The filling time was selected so that the O_3 formation during the following 3-hour UV radiation exposure would coincide with the period of maximum ambient O_3 concentrations at Pasadena and Redlands (Figure S5). Approximately 8 ppb of NO_x (8 ppbv NO_2) and the VOC "mini surrogate"[26,27] (4.4 ppbv ethylene, 2.8 ppbv *n*-hexane, and 0.8 ppbv *m*-xylene) were added to chambers one and three, respectively, by adding 0.8 L of N_2 containing ∼10 ppm of the target compounds at approximately 11 AM. Adding the perturbation gas halfway through the filling procedure encouraged mixing with ambient air in chambers. The small (<0.1%) volume of N_2 added to the 1m^3 total chamber volume makes dilution effects negligible. NO_x, NO_y, O_3, temperature and relative humidity (RH) were measured in each dark chamber after filling for 30 min (10 min for each chamber). UV lights were then turned on for 180 min, while chamber measurements continued in 30 min cycles (10 min for each chamber). The final O_3 concentration in each chamber after 3 h of UV exposure was calculated by fitting a regression curve to the O_3 concentrations during the preceding measurement periods. This approach accounts for changes in the concentration of O_3 that occur during sequential 10 min measurement periods. The difference between final O_3 concentrations in the NO_x-perturbed chamber and the basecase chamber quantified the O_3 sensitivity to NO_x ($\Delta O_3^{+NO_x}$). The difference between the final O_3 concentrations in the VOC-perturbed chamber and the basecase chamber quantified the O_3 sensitivity to VOC (ΔO_3^{+VOC}). The measured O_3 chemical regime was determined by the sign of $\Delta O_3^{+NO_x}$

https://doi.org/10.1021/acsestair.4c00026
ACS EST Air 2024, 1, 536−546

Table 1. Summary of the Measurements in Pasadena and Redlands

No.	instruments	species measured	location	sample duration/ frequency	institution	ref
1	transportable smog chamber system	O_3, NO, NO_2, NOy, Temperature, RH, O_3 sensitivity	Pasadena, Redlands	2 s (O_3), 1 s (others)	UC Davis	7
2	Markes Universal thermal desorption (TD) tube + GC-MS	TO-15 compounds, C3−C5 hydrocarbon	Redlands	10 min, 30 min, 70 min	UC Davis	
3	TD tube + GC-MS	aromatic VOCs, siloxanes, glycols, glycol ethers, and other SVOCs.	Redlands	10 min, 30 min, 70 min	UC Davis	
4	2,4-dinitrophenylhydrazine (DNPH) tube + LC-MS	aldehydes and ketones	Redlands	70 min	UC Davis	
5	CARB PTR-ToF-MS	ethanol, acetonitrile, acetone, acrylonitrile, isoprene, MVK, MEK, benzene, *m*-xylene, α-pinene, 1,2,4-trimethylbenzene, siloxanes	Redlands	1 s	CARB	
6	GC-MS	C2−C10 alkanes, C2−C5 alkenes, acetone, benzene, terpenes, etc.	Pasadena	20 min	NOAA CSL	28
7	I-CIMS	$ClNO_2$, HCOOH, HNO_2, HNO_3, PANs, N_2O_5	Pasadena	1 min	NOAA CSL	29−31
8	CARB mobile platform (Picarro G2401, G2307, G2103)	CO, CO_2, CH_4, H_2O, NH_3, HCHO	Pasadena	1−5 min	CARB	
9	NOAA PTR-ToF-MS	aromatics, monoterpenes, isoprene, OVOCs, siloxanes, etc.	Pasadena	1 s	NOAA CSL	32,33

(positive value = NO_x-limited regime, negative value = VOC-limited regime).

The two smog chamber systems had consistent final O_3 concentration (R^2 = 0.996) and O_3 sensitivity results (R^2 = 0.966) during the co-located tests carried out before and after the main measurement campaign (Figure S7). The initial rate of O_3 formation in the basecase chambers matched the slope of increasing ambient O_3 concentrations at measurement sites (Figure S8), indicating the chamber measurements captured the O_3 chemical formation potential of the ambient air.

2.3. Ambient Measurements. Table 1 shows a full list of ambient measurements made at Pasadena and Redlands during the current study. Detailed descriptions of all the instruments can be found in the Supporting Information. Ambient concentrations of VOCs and other gases (e.g., CO, CH_4, NH_3, etc.) in Pasadena were measured between August 7, 2021 and September 6, 2021, in partnership with the RECAP-CA field campaign. Therefore, VOC measurements in Pasadena are available for only one month. On a subset of study days, offline measurements of BVOCs were augmented with measurements made by the CARB Vocus-Scout Proton-Transfer-Reaction Time-of-Flight Mass Spectrometer (PTR-ToF-MS) that had improved method detection limits relative to offline methods. All ambient measurements in Pasadena and Redlands were averaged between 10 AM and 12 PM (chamber filling period) for the following analysis.

2.4. Chamber Model. A photochemical chamber model[34−36] based on the SAPRC11 chemical mechanism[37] was applied to better understand the response of O_3 to its precursors. The UV spectrum used to calculate photolysis frequencies in the model was adjusted to match the lights used in the chamber.[7] Reaction rate constants were further adjusted based on the measured temperature profile (0−8 °C above ambient due to heat generated by the UV lights in the smog chamber system). Concentrations were initialized using measurements of O_3, NO, NO_2 in the mobile smog chamber systems, and measurements of ambient VOC concentrations. For species that were not measured, concentrations predicted by a chemical transport model (CTM)[38,39] (described in Supporting Information) were used to initialize the chamber model simulations. Uncertainty in CTM-derived species concentrations change predicted chamber model results by less than 7% based on sensitivity tests (Figure S13). Further details of sensitivity tests are listed in Supporting Information. All of the measured ambient VOCs were assigned into the appropriate SAPRC11 species following the rules developed by Carter.[40] Corrections were made for several SAPRC species due to measurement limitations (Figures S9−S12). A full description of the box model setup, a list of measured VOC compounds, and their assigned SAPRC11 species is included in the Supporting Information for both Pasadena and Redlands (Tables S1 and S2).

In this study, the box model simulated the O_3 photochemistry in the basecase and perturbed chambers on all measurement days. The initial concentrations in each simulation reflect the initial concentrations in the chamber. The NO_x-perturbed chamber and the basecase chamber have the same initial VOC concentrations but different initial concentrations of NO, NO_2, and O_3. Temperature and rate constants were updated at 10 min intervals over the 3 h reaction time. The modeled O_3 sensitivity to NO_x was calculated as the difference between O_3 concentrations predicted in the NO_x-perturbed chamber and the basecase chamber.

3. RESULTS AND DISCUSSIONS

3.1. Ambient NO_x, VOC, and O_3 Concentration in SoCAB. Figure 1 shows initial ambient NO_x concentrations, initial VOC level and final basecase chamber O_3 concentrations measured in chamber systems at Pasadena and Redlands. Initial NO_x concentrations were ambient NO_x measurements averaged between 10 AM and 12 PM. Traffic emissions have a large impact on ambient NO_x concentration in the SoCAB.[39,41] The diurnal patterns of measured NO_x concentrations (Figure S14) suggest that partially diluted emissions from traffic influenced initial chamber NO_x concentrations in the current study. NO_x concentrations had greater variability and higher peak values in Pasadena (range from 5−30 ppbv) than in Redlands (below 20 ppbv) (Figure 1a,b). Previous studies have also observed higher NO_x concentrations in Pasadena than Redlands.[9,42]

https://doi.org/10.1021/acsestair.4c00026
ACS EST Air 2024, 1, 536−546

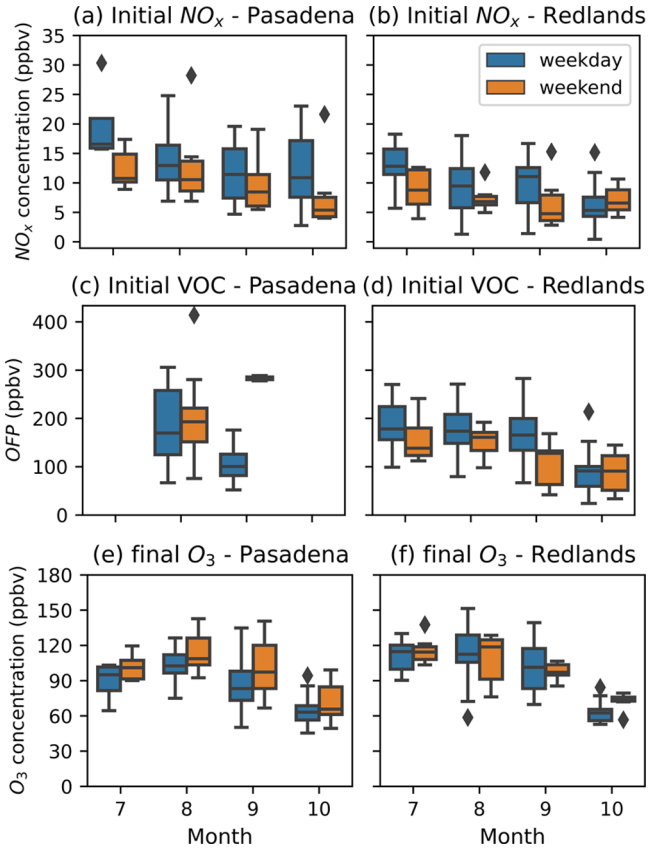

Figure 1. Monthly trend of daily initial NO_x concentration, initial VOC level (represented as OFP) and final O_3 concentration in basecase chamber in Pasadena and Redlands, CA from July to October, 2021. The box shows the quartiles and median of the data set; whiskers show the maximum and minimum of the dataset excluding outliers shown as diamonds.

Measured VOC concentrations are expressed on the basis of their O_3 formation potential (OFP), which is the sum of individual VOC concentrations weighted by their maximum incremental reactivity (MIR).[43,44] VOC concentrations in Pasadena were limited by the number of measurement days. Overall, the measured ranges of VOC concentrations were similar in Pasadena and Redlands. Lower VOC levels were observed in October in Redlands, which likely reflects the seasonal trend in biogenic VOCs.[7] Weekday/weekend changes in VOC levels were not statistically significant except during September 2021 in the Redlands.

The final O_3 concentrations in the basecase chamber were higher than ambient peak O_3 concentrations because atmospheric concentrations undergo dilution as the mixing height increases throughout the day. Chamber concentrations reflect the chemical production of O_3 from reactions of NO_x and VOCs drawn from the atmosphere between 10 AM and 12 PM (Figure S6). Measured final basecase chamber O_3 concentrations in Redlands were greater than or equal to the O_3 concentrations in Pasadena (Figure 1e,f). These chamber results are consistent with trends found in the ambient-temperature O_3 measurements. Redlands has days with maximum 8 h average (MDA8) O_3 larger than 90 ppbv, while all MDA8 O_3 concentrations measured at Pasadena were less than 90 ppbv (Figure S15). Higher MDA8 concentrations of O_3 in the downwind site (Redlands) partially reflects transport of O_3 and its precursors from upwind urban areas in addition to formation of O_3 from local emissions. The formation of O_3 within the chamber system is driven by the reaction of VOCs either emitted locally or transported to the site from upwind sources during the preceding time period. Chamber measurements account for pollutant transport on the day of the experiment up to 12PM when the chamber filling is complete. Transport over the next 3 h is not considered, but agreement between chamber measurements and HCHO/NO_2 values measured by satellites at 1PM each day suggest that the chamber experiment is capturing the dominant factors that determine daily O_3 sensitivity.[7] The different initial NO_x concentrations at Redlands and Pasadena may also influence the chemical regime, which may lead to different levels of the production of O_3 production.

A strong weekday/weekend pattern was observed for NO_x concentrations. The weekend-to-weekday ratio (WE/WD) of initial NO_x was 0.79 in Pasadena and 0.87 in Redlands on average across the entire measurement period. Redlands had higher median weekend NO_x concentrations in October, possibly because the atmosphere happened to be more stagnant on weekends than weekdays during three out of 5 weeks in this month. The effects of this stagnation were also observed at higher ambient temperature on weekends in October. WE/WD trends in NO_x concentrations influence the VOC/NO_x ratio and therefore may modify the O_3 chemical regime.[10,45] Median weekend O_3 concentrations were higher than median weekday O_3 concentrations during all four study months in Pasadena (Figure 1c), suggesting that Pasadena is in the VOC-limited regime. Trends in the Redlands were less obvious, with similar median O_3 concentrations on weekdays and weekends (Figure 1d). The averaged O_3 WE/WD throughout the campaign was observed to be 1.13 in Pasadena and 1.05 in Redlands. The ∼8% weaker O_3 WE/WD at Redlands may be related to the ∼10% weaker NO_x WE/WD at this site. A similar analysis observed WE/WD O_3 equal to 1.38 in Pasadena during CalNex 2010.[10] The weakening of the O_3 weekend effect in Pasadena observed in the current study is consistent with trends observed in a previous study.[46]

3.2. Chamber Measurement of O_3 Sensitivity to NO_x and VOC. Figure 2 shows the sensitivity of the O_3 molecule in the chamber studies carried out in Pasadena and Redlands. Pasadena had a negative median $\Delta O_3^{+NO_x}$ sensitivity throughout the study (Figure 2a). This indicates that the O_3 chemical regime in Pasadena was mostly VOC-limited with very little seasonal trend compared to similar measurements made in Sacramento in 2020 (background boxplot in Figure 2). The upper quartile of $\Delta O_3^{+NO_x}$ was in the NO_x-limited regime on weekends in July and August but quickly transitioned to the VOC-limited regime thereafter. Pasadena is adjacent to the VOC-limited urban core of LA.[7,10] The significant anthropogenic NO_x and VOC emissions in this region are relatively insensitive to temperature-driven seasonal changes (Figure S3) compared to more rural regions with stronger biogenic influence.[7] As expected, ΔO_3^{+VOC} was inversely correlated with $\Delta O_3^{+NO_x}$ in Pasadena. Addition of the VOC surrogate increased the level of O_3 formation by an amount that was greater on weekdays than weekends. The VOC-limited regime in Pasadena has a larger weekend-weekday difference for ΔO_3^{+VOC} than for $\Delta O_3^{+NO_x}$.

Median O_3 sensitivity in Redlands was in the VOC-limited regime in July, transitioned towards the NO_x-limited regime (especially on weekends) during August, and then transitioned back to VOC-limited conditions in September to October. A

https://doi.org/10.1021/acsestair.4c00026
ACS EST Air 2024, 1, 536−546

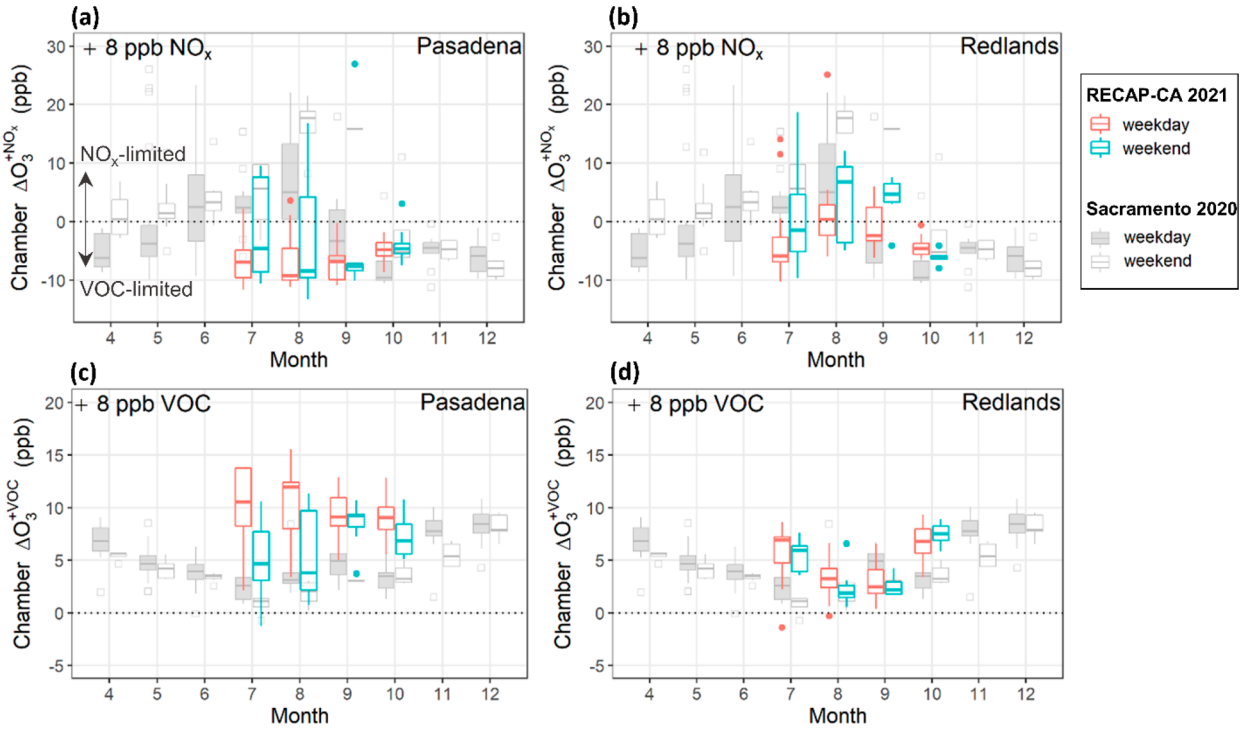

Figure 2. Monthly box-and-whisker plot of O_3 sensitivity measurements ($\Delta O_3^{+NO_x}$ and ΔO_3^{+VOC}) on weekdays and weekends in Pasadena and Redlands, CA from July to October, 2021. The background box-and-whisker plot is the time series of measured O_3 sensitivity in Sacramento, CA in 2020. The box shows the quartiles and median of the dataset, whiskers show the maximum and minimum of the dataset excluding outliers shown as dots.

longer O_3 sensitivity measurement in Sacramento during a previous study year in 2020 (shown as background boxplot in Figure 2) is consistent with this seasonal O_3 sensitivity pattern in Redlands. As was the case in Sacramento, the seasonal change in O_3 sensitivity in Redlands may be influenced by the temperature dependence of biogenic VOC emissions (see isoprene concentration in Figure S12b) and the increased evaporative emissions of semi-volatile organic compounds (SVOCs) on hotter days.[47]

The O_3 sensitivity pattern observed in Pasadena and Redlands reflects the transition from a VOC-limited urban core towards a more NO_x-limited downwind area.[7,21,48,49] Overall, the trends in the O_3 chemical regime observed in Pasadena and Redlands are consistent with recent observations of O_3 chemistry in urban and downwind suburban areas.[7,50]

The days with the highest measured O_3 concentrations are of particular interest in the current study since emissions control programs are traditionally tailored to reduce the O_3 design value, which is determined by the 4th highest MDA8 O_3 averaged over a three-year period. Figure 3 illustrates boxplots of measured $\Delta O_3^{+NO_x}$, and ΔO_3^{+VOC} at Redlands and Pasadena binned according to the MDA8 O_3 concentration measured at nearby monitoring stations.

Pasadena has O_3 sensitivity in the VOC-limited regime on days with MDA8 O_3 < 70 ppbv (Figure 3a). The O_3 chemical regime in Pasadena was evenly distributed between the NO_x-limited regime and VOC-limited regime on days with MDA8 O_3 > 70ppbv. The ΔO_3^{+VOC} (Figure 3c) in Pasadena had an inverse trend compared with the $\Delta O_3^{+NO_x}$. The weakening response of VOC addition on days with higher MDA8 O_3 may be related to higher ambient VOC concentrations (see VOC levels represented as OFP in Figure 5) since the magnitude of the VOC perturbation was constant across all measurements.

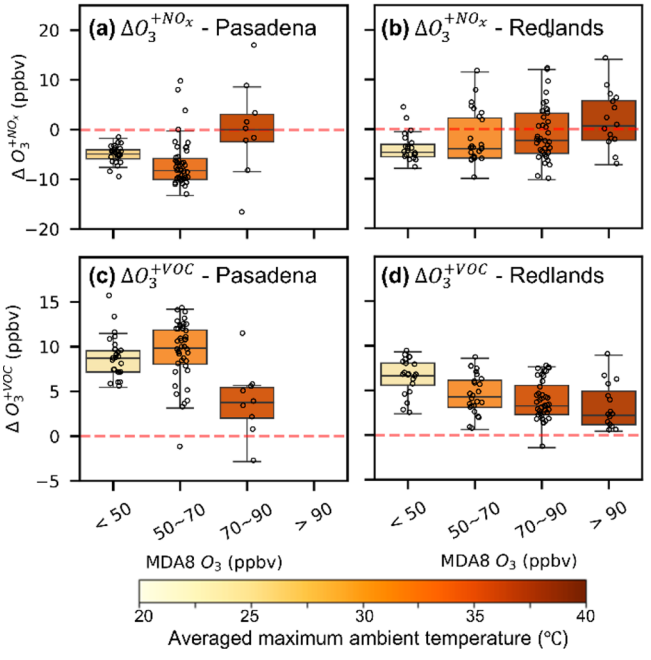

Figure 3. Box-and-whisker plot of the sensitivity of the O_3 to NO_x and VOC as a function of the MDA8 O_3 concentration. Points indicate the data point in each range of the MDA8 O_3 concentration. The color of each box represents daily maximum ambient temperature averaged within that concentration bin.

This may also be caused by increasing loss rates of NO_x under the higher radical production environment on higher MDA8 O_3 days. $\Delta O_3^{+NO_x}$ had greater variability on days with higher MDA8 O_3 than days with lower MDA8 O_3 at Pasadena,

https://doi.org/10.1021/acsestair.4c00026
ACS EST Air 2024, 1, 536−546

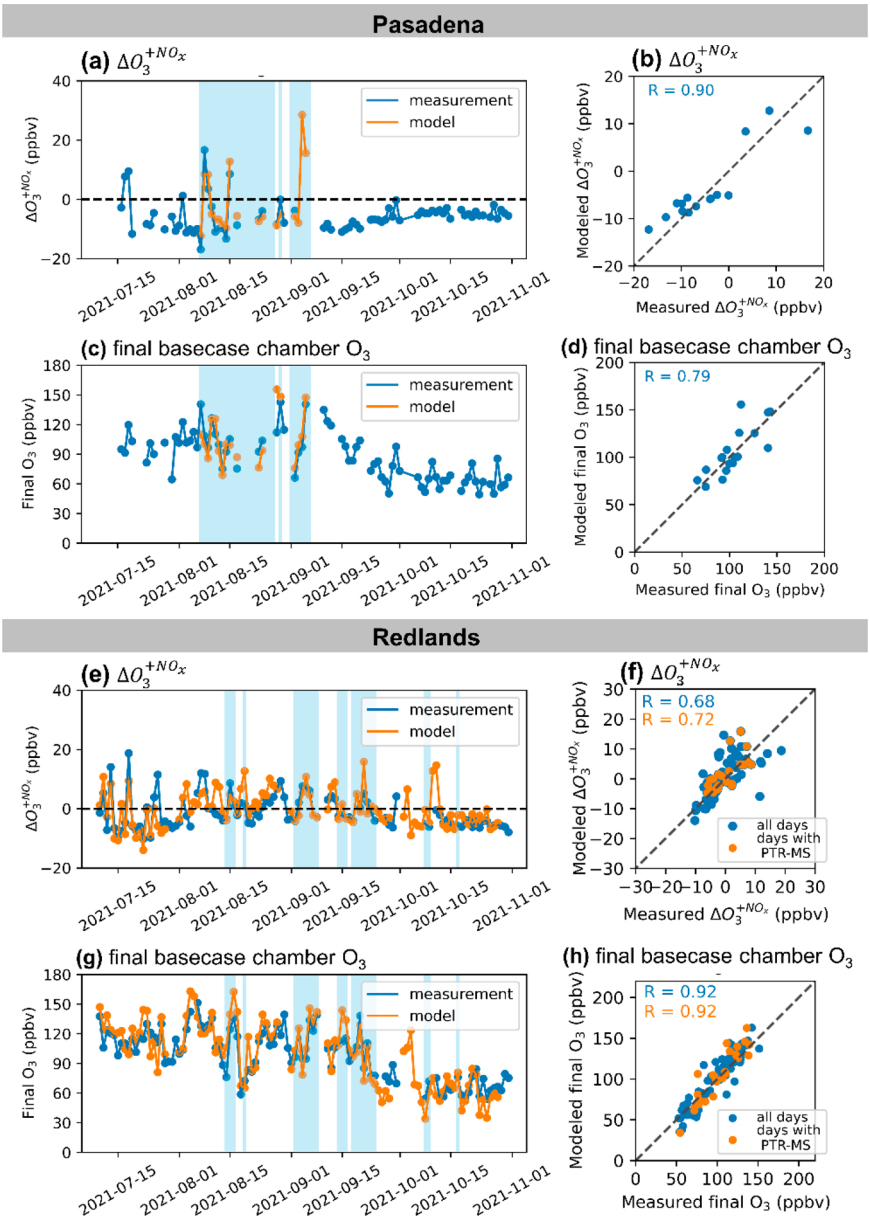

Figure 4. Time series of modeled and measured O_3 concentration and O_3 sensitivity in chambers at Pasadena and Redlands, CA between July and October, 2021. Shaded regions correspond to periods when the most complete VOC measurements were available.

although it should be noted that fewer sample measurements were available in the highest MDA8 O_3 range. Even though median sensitivity was in the transition regime between NO_x-limited and VOC-limited conditions, the sensitivity of the O_3 in Pasadena could be either strongly NO_x-limited or VOC-limited on days with an O_3 concentration above 70 ppbv.

Redlands had negative $\Delta O_3^{+NO_x}$ on more than 90% of days with MDA8 O_3 less than 50 ppbv. As MDA8 concentrations increased, the probability of observing negative $\Delta O_3^{+NO_x}$ decreased. VOC-limited conditions were only measured on 47% of the days with MDA8 O_3 above 90 ppbv (Figure 3b). The trend of more NO_x-limited conditions on higher MDA8 O_3 days in Redlands may be related to both higher VOC emission and higher radical production rates. Variability in $\Delta O_3^{+NO_x}$ increased at higher O_3 concentrations. Overall, Redlands had an almost equal probability of O_3 sensitivity in the VOC-limited (56%) and NO_x-limited (44%) regime on O_3-nonattainment days (MDA8 O_3 > 70 ppbv). The measured O_3 sensitivity trends illustrated in Figure 3 suggest that VOC emission controls should be coupled with NO_x emission controls to mitigate O_3 concentrations at Pasadena and Redlands until NO_x-limited conditions can be achieved.

3.3. Chamber Model Performance. Each chamber experiment was simulated by using a photochemical box model initialized with concentrations that were directly measured and predicted with a regional chemical transport model. Figure 4 shows the predicted/measured final O_3 concentration and $\Delta O_3^{+NO_x}$ at Pasadena and Redlands, respectively. Simulations are restricted to days when VOC measurements were available, which especially restricts the number of days that can be evaluated at Pasadena. Despite the more limited input data, Pasadena simulations span periods with a wide range of O_3 formation and with several transitions between VOC-limited and NO_x-limited conditions. These simulations provide insights into the O_3 sources and chemical regimes at Pasadena even though it was not possible to

https://doi.org/10.1021/acsestair.4c00026
ACS EST Air 2024, 1, 536−546

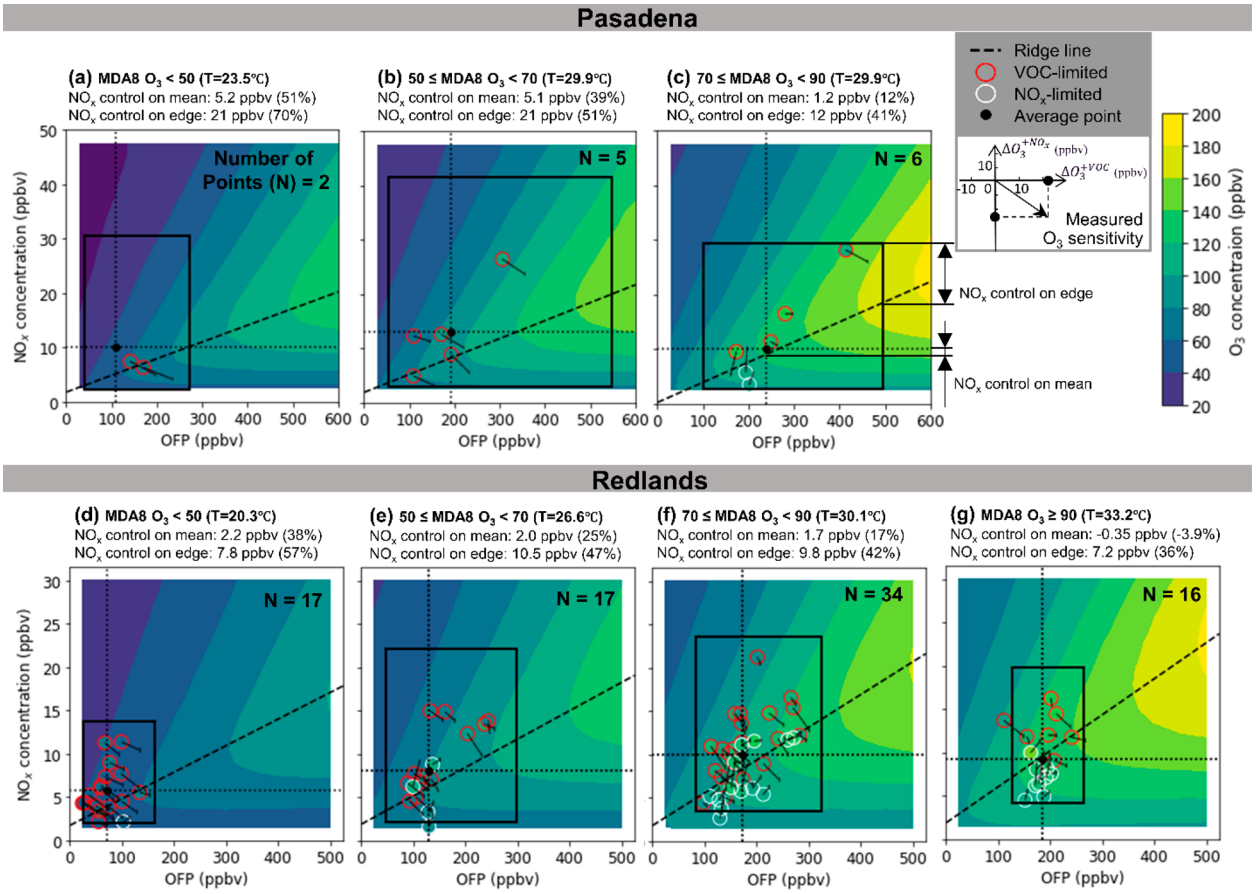

Figure 5. O_3 isopleth at Pasadena (a–c) and Redlands (d–g) over different MDA8 concentration ranges experienced during the study. Dashed ridge lines indicate the transition from NO_x-limited chemistry to VOC-limited chemistry. Also shown are the measured final O_3 concentration (interior dot color shown on concentration key) at measured NO_x and ozone formation potential (OFP) levels. The dotted edge color indicates the measured O_3 chemical regime. The intersection of light dotted lines represents the average measured NO_x and OFP. The arrows on the dot represent the O_3 sensitivity results by combining $\Delta O_3^{+NO_x}$ and ΔO_3^{+VOC}. The box around the average represents the 95% confidence interval of the measured values.

simulate the transition into the fall season. Simulations at Redlands span the full measurement time period, tracking the seasonal decline in base concentrations of O_3 and multiple transitions between VOC-limited and NO_x-limited regimes. Days with the most complete initial VOC data including PTR-ToF-MS measurements (blue shading) have higher correlation (R value) between model predictions and measurements. Overall, the good correlation between predicted and measured final O_3 concentration in the basecase chamber and $\Delta O_3^{+NO_x}$ in the perturbed chamber shows that the box model can reproduce the behavior of the chamber experiments at Pasadena and Redlands. NO_y concentrations predicted by model calculations were also in good agreement with chamber measurement (Figure S16). Sensitivity tests show that use of chamber temperature vs ambient temperature has little influence on the comparison between predicted and measured final O_3 concentration in the basecase chamber and $\Delta O_3^{+NO_x}$ in the perturbed chamber (Figures S17 and S18). Ambient temperature profiles are therefore used to predict the O_3 isopleth in the remainder of the analysis.

3.4. Measured O_3 Sensitivity on Modeled O_3 Isopleth.

O_3 isopleth diagrams summarize the nonlinear relationship between O_3 formation of the o_3 and precursor NO_x/VOC concentrations. Traditional O_3 isopleth diagrams are based exclusively on model predictions. In the current study, it is possible to add direct measurements of O_3 sensitivity to the isopleths calculated with the chamber model in order to verify both the base O_3 concentration and the response in O_3 concentrations caused by perturbations in NO_x/VOC levels.

O_3 isopleths were generated each day by simulating the O_3 formation at multiple scaled NO_x and VOCs levels around the base concentrations measured for that day. Measured VOC concentrations are expressed on the basis of their O_3 formation potential (OFP), which is the sum of individual VOC concentrations weighted by their maximum incremental reactivity (MIR).[43,44] Separate isopleths are averaged based on the MDA8 O_3 range. Each averaged O_3 isopleth in Figure 5 therefore represents the averaged O_3 chemistry for multiple days within the target MDA8 concentration range. Increasing MDA8 concentrations generally correspond to higher average temperature (values in each subpanel title).

Measured final O_3 concentrations are plotted as open circles in Figure 5 by using the same color key as the modeled O_3 isopleth. The number of measurement points is restricted to days when NO_x, VOC, and O_3 sensitivity measurements were all available. The location of each observation circle is based on the measured NO_x and VOC concentrations. Most measurements of final concentrations of O_3 are in good agreement with model predictions, as indicated by the similarity between the color of each circle and the background color of the isopleth.

https://doi.org/10.1021/acsestair.4c00026
ACS EST Air 2024, 1, 536–546

The measured O_3 chemical regime is indicated by the outline color of each dot (red: VOC-limited regime; white: NO_x-limited regime). Most of the measurements match the O_3 sensitivity regime in the predicted O_3 isopleth. The few measurement points that fall in the wrong O_3 sensitivity regime in Figure 5 are located in the transition regime (very close to the ridge line). The white dots (measured with NO_x-limited chemistry) on the wrong side of the isopleth ridgeline have greater error than red dots (measured with VOC-limited chemistry) on the wrong side of the ridgeline. The white dots may have greater uncertainty due to an underestimation of the VOC level in the box model. The arrow attached to each measurement point indicates the measured sensitivity to NO_x and VOC perturbation ($\Delta O_3^{+NO_x}$ and ΔO_3^{+VOC}). Arrows pointing to the bottom-right indicate that the addition of NO_x decreased the O_3 concentration, while arrows pointing to the upper-right indicate that the addition of NO_x increased the O_3 concentrations. Arrows should be orthogonal to the background isopleth lines. Overall, the generally accurate model performance over most of the study period supports a deeper understanding of the O_3 precursors and control program design.

The average NO_x and VOC concentrations measured during the study period are shown at the intersection of the dotted lines in Figures 5. Average VOC concentrations were higher on days with higher MDA8 O_3 (and temperature). Average O_3 sensitivity in Pasadena is slightly NO_x-limited on the days of O_3-nonattainment days. Averaged O_3 sensitivity in Redlands is slightly VOC-limited on days with MDA8 O_3 between 70−90 ppbv, and NO_x-limited on days with MDA8 O_3 > 90 ppbv. The averaged O_3 sensitivity calculated in each O_3 isopleth has the same O_3 sensitivity regime as the median measurements summarized in Figure 3.

The vertical distance between the intersection of the dotted lines to the ridge line in Figure 5 indicates the amount of NO_x reduction that is needed to reach NO_x-limited conditions for the averaged O_3 sensitivity regime based on the composition of the atmosphere between 10 AM to 12 PM. NO_x concentrations in Pasadena would need to be reduced by 12% (assuming VOC is stable) before the average O_3 chemical regime reaches NO_x-limited conditions on O_3-nonattainment days. NO_x concentrations in Redlands would need to be reduced by 17% before the average O_3 chemical regime reached NO_x-limited conditions in Redlands when MDA8 O_3 is between 70−90 ppbv.

Each confidence interval box shown in Figure 5 assumes that the NO_x and OFP concentrations follow a log-normal distribution.[51] The interior region of the black box represents the O_3 chemistry, corresponding to 95% of the ambient measurements. All of the NO_x and VOC measurements available during the experimental window were used to calculate the confidence intervals in order to maximize the sample size. The NO_x confidence intervals in Pasadena and Redlands were based on 80 and 100 days of ambient measurements, respectively. The OFP confidence interval was based on 30 days of VOC measurements in Pasadena and 100 days of VOC measurements in Redlands. The vertical distance between the upper-right edge of the confidence interval to the ridge line represents the amount of NO_x control needed to move 95% of the observations with the highest O_3 concentrations to the NO_x-limited chemical regime in the absence of any VOC controls. The calculations summarized in Figure 5 indicate that NO_x concentrations need to decrease by ~40% in order to reach the NO_x-limited condition on 95% of the days at Pasadena and Redlands based on the composition of the atmosphere between 10 AM to 12 PM. It should be noted that the 40% NO_x reduction only barely reaches the NO_x-limited regime on peak O_3 days. Further NO_x control is still needed to reduce the O_3 design values. Perdigones et al.[49] reported a comparable or larger amount of NO_x reduction (40−60%) in the SoCAB that could reduce the number of O_3-nonattainment days to 20−10%. The State Implementation Plan from SCAQMD[8] estimated that a 67% NO_x reduction would be needed in the SoCAB to comply with the O_3 NAAQS by 2037. All of the evidence suggests that NO_x reductions greater than 40% are required to control the concentration of the O_3 in the SoCAB.

The control of VCPs may reduce ambient O_3 concentrations, as recent studies[18,19,52] have found that VCPs make significant contributions to the anthropogenic VOC emissions that contribute to O_3 formation in urban areas. Tagged CTM calculations[53] and receptor-oriented source apportionment calculations[54] show that biogenic VOCs are present at sufficiently high concentrations to prevent full compliance with the O_3 NAAQS in Southern California based on a VOC-control program alone. Future work[54] will publish VOC source apportionment results to better understand appropriate levels of anthropogenic VOC emissions perturbations, but this analysis is beyond the reasonable scope of the current study.

While the O_3 isopleths predicted in the current study are consistent with multiple observations, limitations in both measurements and model calculations should be noted. The chamber methods used in the current study quantify the chemical production of O_3 but do not consider the effects of dilution, mixing, and deposition processes. The chamber measurements focus on the time of day that characterizes peak O_3 production that is relevant for the design of the O_3 control programs, but measurements were not made at other times of the day that may fall into different chemical regimes. Other factors (e.g., UV radiation, temperature, amount of NO_x/VOC perturbations) investigated in a previous study[7] were found to have limited impact on the chamber results. Box-model calculations carried out to gain a deeper understanding of the measurements suggest that these issues do not alter the overall conclusions of the study, but those same box model calculations have uncertainty associated with initial VOC concentrations on days when only partial measurements were available. The latest version of the chemical mechanism (e.g., SAPRC22) includes more explicit organic compounds and chemical reactions that theoretically improve the representation of photochemistry compared to earlier versions. Venecek et al. (2018) determined that SAPRC11 had superior performance when predicting ambient ozone concentrations across California compared to SAPRC16 (the immediate predecessor to SAPRC18 and SAPRC22). The use of SAPRC11 vs SAPRC22 does not significantly affect the results or conclusions of the current study. Overall, the novel comparisons between measurements and model predictions improve our understanding and confidence in the emissions control programs designed to reduce O_3 concentrations in Southern California.

The findings in the current study help to explain the atmospheric impacts of the COVID-19 stay-at-home order in California (March to June, 2020) that decreased traffic by as much as 50% in the SoCAB.[21,55] NO_x concentrations

https://doi.org/10.1021/acsestair.4c00026
ACS EST Air 2024, 1, 536−546

decreased by 26% in Pasadena and 8% in Redlands as a result.[14]

Parker et al.[14] analyzed ambient data and concluded that the western portion of the SoCAB remained VOC-limited despite these significant reductions in ambient NO_x concentrations. Likewise, the results of the current study indicate that the urban cores of major cities in Los Angeles remain VOC-limited in all seasons.[7] This further supports the conclusions of the current analysis that ~30% NO_x reductions are not sufficient to transition to the NO_x-limited regime and consequently reduce O_3 concentrations in polluted urban core areas in the SoCAB. Additional analyses compared the ambient air quality data between the weekdays and weekends that experience natural variabilities in traffic activities as an alternative approach to understanding the O_3 sensitivities in the SoCAB.[21] However, the results did not pass statistical confidence measures (see Supporting Information) due to the low number of data points available for comparison during the heavily modified traffic conditions following the stay-at-home order. The inconsistencies in meteorological conditions also contributed to significant uncertainties in this analysis. This demonstrates the strength and the need for tools used in this study that yield an understanding of the chemistry of the O_3 regimes at daily intervals.

■ ASSOCIATED CONTENT

Supporting Information

The Supporting Information is available free of charge at https://pubs.acs.org/doi/10.1021/acsestair.4c00026.

Additional experimental details, materials, results, and methods, including map of field sites, meteorological and ambient NO_x and O_3 trend, transportable smog chamber measurements design, descriptions of ambient measurement instruments, lists of all measured VOCs and their statistics, and box model setup, performance and uncertainty analysis (PDF)

■ AUTHOR INFORMATION

Corresponding Author

Michael J. Kleeman − *Department of Civil and Environmental Engineering, UC Davis, Davis, California 95616, United States;* orcid.org/0000-0002-0347-7512; Email: mjkleeman@ucdavis.edu

Authors

Shenglun Wu − *Department of Civil and Environmental Engineering, UC Davis, Davis, California 95616, United States*

Christopher P. Alaimo − *Department of Civil and Environmental Engineering, UC Davis, Davis, California 95616, United States*

Yusheng Zhao − *Department of Civil and Environmental Engineering, UC Davis, Davis, California 95616, United States;* orcid.org/0000-0002-4575-9438

Peter G. Green − *Department of Civil and Environmental Engineering, UC Davis, Davis, California 95616, United States*

Thomas M. Young − *Department of Civil and Environmental Engineering, UC Davis, Davis, California 95616, United States;* orcid.org/0000-0001-7217-4753

Shang Liu − *California Air Resources Board, Sacramento, California 95814, United States;* Present Address: Department of Civil and Environmental Engineering, Northeastern University, Boston, MA 02115, U.S.A

Toshihiro Kuwayama − *California Air Resources Board, Sacramento, California 95814, United States;* orcid.org/0000-0002-0540-0156

Matthew M. Coggon − *Chemical Sciences Laboratory, National Oceanic and Atmospheric Administration, Boulder, Colorado 80305, United States;* orcid.org/0000-0002-5763-1925

Chelsea E. Stockwell − *Chemical Sciences Laboratory, National Oceanic and Atmospheric Administration, Boulder, Colorado 80305, United States; Cooperative Institute for Research in Environmental Sciences, University of Colorado−Boulder, Boulder, Colorado 80309, United States;* orcid.org/0000-0003-3462-2126

Lu Xu − *Chemical Sciences Laboratory, National Oceanic and Atmospheric Administration, Boulder, Colorado 80305, United States; Cooperative Institute for Research in Environmental Sciences, University of Colorado−Boulder, Boulder, Colorado 80309, United States;* Present Address: Department of Energy, Environmental and Chemical Engineering, Washington University in St. Louis, Missouri, U.S.A.; orcid.org/0000-0002-0021-9876

Carsten Warneke − *Chemical Sciences Laboratory, National Oceanic and Atmospheric Administration, Boulder, Colorado 80305, United States;* orcid.org/0000-0003-3811-8496

Jessica B. Gilman − *Chemical Sciences Laboratory, National Oceanic and Atmospheric Administration, Boulder, Colorado 80305, United States;* orcid.org/0000-0002-7899-9948

Michael A. Robinson − *Chemical Sciences Laboratory, National Oceanic and Atmospheric Administration, Boulder, Colorado 80305, United States; Cooperative Institute for Research in Environmental Sciences, University of Colorado−Boulder, Boulder, Colorado 80309, United States*

Patrick R. Veres − *Chemical Sciences Laboratory, National Oceanic and Atmospheric Administration, Boulder, Colorado 80305, United States;* Present Address: National Center for Atmospheric Research, Boulder, Colorado, U.S.A.

□**J. Andrew Neuman** − *Chemical Sciences Laboratory, National Oceanic and Atmospheric Administration, Boulder, Colorado 80305, United States; Cooperative Institute for Research in Environmental Sciences, University of Colorado−Boulder, Boulder, Colorado 80309, United States*

Complete contact information is available at: https://pubs.acs.org/10.1021/acsestair.4c00026

Notes

The authors declare no competing financial interest.

□Retired.

■ ACKNOWLEDGMENTS

This research was supported by the California Air Resources Board (Grant No. 19RD012), the Coordinating Research Council (Grant Nos. A-121 and A-121-2), and the University of California Institute of Transportation Studies through funding from the State of California via the Public Transportation Account and the Road Repair and Accountability Act of 2017 (SB 1). The NOAA Chemical Sciences Laboratory acknowledges support for this work from the California Air Resources Board under Agreement Number 20RD002. This

work was supported in part by the NOAA Cooperative Agreement with CIRES, NA17OAR4320101. The authors thank Albert Dietrich at the SCAQMD for help with site preparation and access during sample collection at Redlands as part of the RECAP-CA field study. We also thank the CIT research team (Paul Wennberg, John Seinfeld, Benjamin Schulze, and Ryan Ward) for hosting the RECAP-CA field study.

REFERENCES

(1) Sillman, S.; Logan, J. A.; Wofsy, S. C. The Sensitivity of Ozone to Nitrogen Oxides and Hydrocarbons in Regional Ozone Episodes. *J. Geophys. Res. Atmospheres* **1990**, *95* (D2), 1837−1851.
(2) Seinfeld, J. H. *Atmospheric Chemistry and Physics: From Air Pollution to Climate Change*, 3rd ed.; John Wiley & Sons: Hoboken, NJ, 2016.
(3) Ryerson, T. B.; Andrews, A. E.; Angevine, W. M.; Bates, T. S.; Brock, C. A.; Cairns, B.; Cohen, R. C.; Cooper, O. R.; De Gouw, J. A.; Fehsenfeld, F. C.; Ferrare, R. A.; Fischer, M. L.; Flagan, R. C.; Goldstein, A. H.; Hair, J. W.; Hardesty, R. M.; Hostetler, C. A.; Jimenez, J. L.; Langford, A. O.; McCauley, E.; McKeen, S. A.; Molina, L. T.; Nenes, A.; Oltmans, S. J.; Parrish, D. D.; Pederson, J. R.; Pierce, R. B.; Prather, K.; Quinn, P. K.; Seinfeld, J. H.; Senff, C. J.; Sorooshian, A.; Stutz, J.; Surratt, J. D.; Trainer, M.; Volkamer, R.; Williams, E. J.; Wofsy, S. C. The 2010 California Research at the Nexus of Air Quality and Climate Change (CalNex) Field Study. *J. Geophys. Res. Atmospheres* **2013**, *118* (11), 5830−5866.
(4) Pollack, I. B.; Ryerson, T. B.; Trainer, M.; Neuman, J. A.; Roberts, J. M.; Parrish, D. D. Trends in Ozone, Its Precursors, and Related Secondary Oxidation Products in Los Angeles, California: A Synthesis of Measurements from 1960 to 2010. *J. Geophys. Res. Atmospheres* **2013**, *118* (11), 5893−5911.
(5) Parrish, D. D.; Xu, J.; Croes, B.; Shao, M. Air Quality Improvement in Los Angeles—Perspectives for Developing Cities. *Front. Environ. Sci. Eng.* **2016**, *10* (5), na DOI: 10.1007/s11783-016-0859-5.
(6) Fujita, E. M.; Campbell, D. E.; Stockwell, W. R.; Lawson, D. R. Past and Future Ozone Trends in California's South Coast Air Basin: Reconciliation of Ambient Measurements with Past and Projected Emission Inventories. *J. Air Waste Manag. Assoc.* **2013**, *63* (1), 54−69.
(7) Wu, S.; Lee, H. J.; Anderson, A.; Liu, S.; Kuwayama, T.; Seinfeld, J. H.; Kleeman, M. J. Direct Measurements of Ozone Response to Emissions Perturbations in California. *Atmospheric Chem. Phys.* **2022**, *22* (7), 4929−4949.
(8) South Coast AQMD. *South Coast Air Quality Management District 2022 Air Quality Management Plan*, 2022.
(9) Nussbaumer, C. M.; Cohen, R. C. The Role of Temperature and NO Xin Ozone Trends in the Los Angeles Basin. *Environ. Sci. Technol.* **2020**, *54* (24), 15652−15659.
(10) Pollack, I. B.; Ryerson, T. B.; Trainer, M.; Parrish, D. D.; Andrews, A. E.; Atlas, E. L.; Blake, D. R.; Brown, S. S.; Commane, R.; Daube, B. C.; De Gouw, J. A.; Dubé, W. P.; Flynn, J.; Frost, G. J.; Gilman, J. B.; Grossberg, N.; Holloway, J. S.; Kofler, J.; Kort, E. A.; Kuster, W. C.; Lang, P. M.; Lefer, B.; Lueb, R. A.; Neuman, J. A.; Nowak, J. B.; Novelli, P. C.; Peischl, J.; Perring, A. E.; Roberts, J. M.; Santoni, G.; Schwarz, J. P.; Spackman, J. R.; Wagner, N. L.; Warneke, C.; Washenfelder, R. A.; Wofsy, S. C.; Xiang, B. Airborne and Ground-Based Observations of a Weekend Effect in Ozone, Precursors, and Oxidation Products in the California South Coast Air Basin. *J. Geophys. Res. Atmospheres* **2012**, *117* (3), 1−14.
(11) Fujita, E. M.; Campbell, D. E.; Stockwell, W. R.; Saunders, E.; Fitzgerald, R.; Perea, R. Projected Ozone Trends and Changes in the Ozone-Precursor Relationship in the South Coast Air Basin in Response to Varying Reductions of Precursor Emissions. *J. Air Waste Manag. Assoc.* **2016**, *66* (2), 201−214.
(12) Warneke, C.; De Gouw, J. A.; Edwards, P. M.; Holloway, J. S.; Gilman, J. B.; Kuster, W. C.; Graus, M.; Atlas, E.; Blake, D.; Gentner, D. R.; Goldstein, A. H.; Harley, R. A.; Alvarez, S.; Rappenglueck, B.; Trainer, M.; Parrish, D. D. Photochemical Aging of Volatile Organic Compounds in the Los Angeles Basin: Weekday-Weekend Effect. *J. Geophys. Res. Atmospheres* **2013**, *118* (10), 5018−5028.
(13) Rasmussen, D. J.; Hu, J.; Mahmud, A.; Kleeman, M. J. The Ozone-Climate Penalty: Past, Present, and Future. *Environ. Sci. Technol.* **2013**, *47* (24), 14258−14266.
(14) Parker, H. A.; Hasheminassab, S.; Crounse, J. D.; Roehl, C. M.; Wennberg, P. O. Impacts of Traffic Reductions Associated With COVID-19 on Southern California Air Quality. *Geophys. Res. Lett.* **2020**, *47* (23), 1−9.
(15) Chossière, G. P.; Xu, H.; Dixit, Y.; Isaacs, S.; Eastham, S. D.; Allroggen, F.; Speth, R. L.; Barrett, S. R. H. Air Pollution Impacts of COVID-19−Related Containment Measures. *Sci. Adv.* **2021**, *7* (21), na.
(16) Lee, J. D.; Drysdale, W. S.; Finch, D. P.; Wilde, S. E.; Palmer, P. I. UK Surface NO2 Levels Dropped by 42 % during the COVID-19 Lockdown: Impact on Surface O3. *Atmospheric Chem. Phys.* **2020**, *20* (24), 15743−15759.
(17) Kroll, J. H.; Heald, C. L.; Cappa, C. D.; Farmer, D. K.; Fry, J. L.; Murphy, J. G.; Steiner, A. L. The Complex Chemical Effects of COVID-19 Shutdowns on Air Quality. *Nat. Chem.* **2020**, *12* (9), 777−779.
(18) McDonald, B. C.; De Gouw, J. A.; Gilman, J. B.; Jathar, S. H.; Akherati, A.; Cappa, C. D.; Jimenez, J. L.; Lee-Taylor, J.; Hayes, P. L.; McKeen, S. A.; Cui, Y. Y.; Kim, S. W.; Gentner, D. R.; Isaacman-VanWertz, G.; Goldstein, A. H.; Harley, R. A.; Frost, G. J.; Roberts, J. M.; Ryerson, T. B.; Trainer, M. Volatile Chemical Products Emerging as Largest Petrochemical Source of Urban Organic Emissions. *Science* **2018**, *359* (6377), 760−764.
(19) Coggon, M. M.; Gkatzelis, G. I.; McDonald, B. C.; Gilman, J. B.; Schwantes, R. H.; Abuhassan, N.; Aikin, K. C.; Arend, M. F.; Berkoff, T. A.; Brown, S. S.; Campos, T. L.; Dickerson, R. R.; Gronoff, G.; Hurley, J. F.; Isaacman-Vanwertz, G.; Koss, A. R.; Li, M.; McKeen, S. A.; Moshary, F.; Peischl, J.; Pospisilova, V.; Ren, X.; Wilson, A.; Wu, Y.; Trainer, M.; Warneke, C. Volatile Chemical Product Emissions Enhance Ozone and Modulate Urban Chemistry. *Proc. Natl. Acad. Sci. U. S. A.* **2021**, *118* (32), na.
(20) Gkatzelis, G. I.; Coggon, M. M.; McDonald, B. C.; Peischl, J.; Gilman, J. B.; Aikin, K. C.; Robinson, M. A.; Canonaco, F.; Prevot, A. S. H.; Trainer, M.; Warneke, C. Observations Confirm That Volatile Chemical Products Are a Major Source of Petrochemical Emissions in U.S. Cities. *Environ. Sci. Technol.* **2021**, *55* (8), 4332−4343.
(21) Schroeder, J. R.; Cai, C.; Xu, J.; Ridley, D.; Lu, J.; Bui, N.; Yan, F.; Avise, J. Changing Ozone Sensitivity in the South Coast Air Basin during the COVID-19 Period. *Atmospheric Chem. Phys.* **2022**, *22* (19), 12985−13000.
(22) Cardelino, C. A.; Chameides, W. L. An Observation-Based Model for Analyzing Ozone Precursor Relationships in the Urban Atmosphere. *J. Air Waste Manag. Assoc.* **1995**, *45* (3), 161−180.
(23) Wolfe, G. M.; Marvin, M. R.; Roberts, S. J.; Travis, K. R.; Liao, J. The Framework for 0-D Atmospheric Modeling (F0AM) v3.1. *Geosci. Model Dev.* **2016**, *9* (9), 3309−3319.
(24) Abdi-Oskouei, M.; Roozitalab, B.; Stanier, C. O.; Christiansen, M.; Pfister, G.; Pierce, R. B.; McDonald, B. C.; Adelman, Z.; Janseen, M.; Dickens, A. F.; Carmichael, G. R. The Impact of Volatile Chemical Products, Other VOCs, and NOx on Peak Ozone in the Lake Michigan Region. *J. Geophys. Res. Atmospheres* **2022**, *127* (22), No. e2022JD037042.
(25) Meteorology Data Query Tool (PST). https://www.arb.ca.gov/aqmis2/metselect.php (accessed 2024-01-17).
(26) Carter, W.; Luo, D.; Malkina, I.; Pierce, J. *Environmental Chamber Studies of Atmospheric Reactivities of Volatile Organic Compounds: Effects of Varying Chamber and Light Source*; National Renewable Energy Laboratory, 1995. DOI: 10.2172/57153.
(27) Carter, W. P. L.; Pierce, J. A.; Luo, D.; Malkina, I. L. Environmental Chamber Study of Maximum Incremental Reactivities of Volatile Organic Compounds. *Atmos. Environ.* **1995**, *29* (18), 2499−2511.

(28) Lerner, B. M.; Gilman, J. B.; Aikin, K. C.; Atlas, E. L.; Goldan, P. D.; Graus, M.; Hendershot, R.; Isaacman-VanWertz, G. A.; Koss, A.; Kuster, W. C.; Lueb, R. A.; McLaughlin, R. J.; Peischl, J.; Sueper, D.; Ryerson, T. B.; Tokarek, T. W.; Warneke, C.; Yuan, B.; de Gouw, J. A. An Improved, Automated Whole Air Sampler and Gas Chromatography Mass Spectrometry Analysis System for Volatile Organic Compounds in the Atmosphere. *Atmospheric Meas. Technol.* **2017**, *10* (1), 291−313.
(29) Veres, P. R.; Neuman, J. A.; Bertram, T. H.; Assaf, E.; Wolfe, G. M.; Williamson, C. J.; Weinzierl, B.; Tilmes, S.; Thompson, C. R.; Thames, A. B.; Schroder, J. C.; Saiz-Lopez, A.; Rollins, A. W.; Roberts, J. M.; Price, D.; Peischl, J.; Nault, B. A.; Møller, K. H.; Miller, D. O.; Meinardi, S.; Li, Q.; Lamarque, J. F.; Kupc, A.; Kjaergaard, H. G.; Kinnison, D.; Jimenez, J. L.; Jernigan, C. M.; Hornbrook, R. S.; Hills, A.; Dollner, M.; Day, D. A.; Cuevas, C. A.; Campuzano-Jost, P.; Burkholder, J.; Bui, T. P.; Brune, W. H.; Brown, S. S.; Brock, C. A.; Bourgeois, I.; Blake, D. R.; Apel, E. C.; Ryerson, T. B. Global Airborne Sampling Reveals a Previously Unobserved Dimethyl Sulfide Oxidation Mechanism in the Marine Atmosphere. *Proc. Natl. Acad. Sci. U. S. A.* **2020**, *117* (9), 4505−4510.
(30) Veres, P. R.; Roberts, J. M. Development of a Photochemical Source for the Production and Calibration of Acyl Peroxynitrate Compounds. *Atmospheric Meas. Technol.* **2015**, *8* (5), 2225−2231.
(31) Robinson, M. A.; Neuman, J. A.; Huey, L. G.; Roberts, J. M.; Brown, S. S.; Veres, P. R. Temperature-Dependent Sensitivity of Iodide Chemical Ionization Mass Spectrometers. *Atmospheric Meas. Technol.* **2022**, *15* (14), 4295−4305.
(32) Krechmer, J.; Lopez-Hilfiker, F.; Koss, A.; Hutterli, M.; Stoermer, C.; Deming, B.; Kimmel, J.; Warneke, C.; Holzinger, R.; Jayne, J.; Worsnop, D.; Fuhrer, K.; Gonin, M.; De Gouw, J. Evaluation of a New Reagent-Ion Source and Focusing Ion-Molecule Reactor for Use in Proton-Transfer-Reaction Mass Spectrometry. *Anal. Chem.* **2018**, *90* (20), 12011−12018.
(33) Coggon, M. M.; Stockwell, C. E.; Claflin, M. S.; Pfannerstill, E. Y.; Xu, L.; Gilman, J. B.; Marcantonio, J.; Cao, C.; Bates, K.; Gkatzelis, G. I.; Lamplugh, A.; Katz, E. F.; Arata, C.; Apel, E. C.; Hornbrook, R. S.; Piel, F.; Majluf, F.; Blake, D. R.; Wisthaler, A.; Canagaratna, M.; Lerner, B. M.; Goldstein, A. H.; Mak, J. E.; Warneke, C. Identifying and Correcting Interferences to PTR-ToF-MS Measurements of Isoprene and Other Urban Volatile Organic Compounds. *Atmospheric Meas. Technol.* **2024**, *17* (2), 801−825.
(34) Howard, C. J.; Yang, W.; Green, P. G.; Mitloehner, F.; Malkina, I. L.; Flocchini, R. G.; Kleeman, M. J. Direct Measurements of the Ozone Formation Potential from Dairy Cattle Emissions Using a Transportable Smog Chamber. *Atmos. Environ.* **2008**, *42* (21), 5267−5277.
(35) Howard, C. J.; Kumar, A.; Mitloehner, F.; Stackhouse, K.; Green, P. G.; Flocchini, R. G.; Kleeman, M. J. Direct Measurements of the Ozone Formation Potential from Livestock and Poultry Waste Emissions. *Environ. Sci. Technol.* **2010**, *44* (7), 2292−2298.
(36) Howard, C. J.; Kumar, A.; Malkina, I.; Mitloehner, F.; Green, P. G.; Flocchini, R. G.; Kleeman, M. J. Reactive Organic Gas Emissions from Livestock Feed Contribute Significantly to Ozone Production in Central California. *Environ. Sci. Technol.* **2010**, *44* (7), 2309−2314.
(37) Carter, W. P. L.; Heo, G. Development of Revised SAPRC Aromatics Mechanisms. *Atmos. Environ.* **2013**, *77*, 404−414.
(38) Kleeman, M. J.; Cass, G. R. A 3D Eulerian Source-Oriented Model for an Externally Mixed Aerosol. *Environ. Sci. Technol.* **2001**, *35* (24), 4834−4848.
(39) Zhao, Y.; Li, Y.; Kumar, A.; Ying, Q.; Vandenberghe, F.; Kleeman, M. J. Separately Resolving NOx and VOC Contributions to Ozone Formation. *Atmos. Environ.* **2022**, *285*, 119224−119224.
(40) Carter, W. P. L. Development of a Database for Chemical Mechanism Assignments for Volatile Organic Emissions. *J. Air Waste Manag. Assoc.* **2015**, *65* (10), 1171−1184.
(41) Liu, J.; Lipsitt, J.; Jerrett, M.; Zhu, Y. Decreases in Near-Road NO and NO2Concentrations during the COVID-19 Pandemic in California. *Environ. Sci. Technol. Lett.* **2021**, *8* (2), 161.
(42) Russell, A. R.; Valin, L. C.; Bucsela, E. J.; Wenig, M. O.; Cohen, R. C. Space-Based Constraints on Spatial and Temporal Patterns of NOx Emissions in California, 2005−2008. *Environ. Sci. Technol.* **2010**, *44* (9), 3608−3615.
(43) Carter, W. P. L. Updated Maximum Incremental Reactivity Scale and Hydrocarbon Bin Reactivities for Regulatory Applications. *Calif. Air Resour. Board Contract* **2009**, 339−339.
(44) Venecek, M. A.; Cai, C.; Kaduwela, A.; Avise, J.; Carter, W. P. L.; Kleeman, M. J. Analysis of SAPRC16 Chemical Mechanism for Ambient Simulations. *Atmos. Environ.* **2018**, *192*, 136−150.
(45) Fujita, E. M.; Stockwell, W. R.; Campbell, D. E.; Keislar, R. E.; Lawson, D. R. Evolution of the Magnitude and Spatial Extent of the Weekend Ozone Effect in California's South Coast Air Basin, 1981−2000. *J. Air Waste Manag. Assoc.* **2003**, *53* (7), 802−815.
(46) Baidar, S.; Hardesty, R. M.; Kim, S. W.; Langford, A. O.; Oetjen, H.; Senff, C. J.; Trainer, M.; Volkamer, R. Weakening of the Weekend Ozone Effect over California's South Coast Air Basin. *Geophys. Res. Lett.* **2015**, *42* (21), 9457−9464.
(47) Pusede, S. E.; Steiner, A. L.; Cohen, R. C. Temperature and Recent Trends in the Chemistry of Continental Surface Ozone. *Chem. Rev.* **2015**, *115* (10), 3898−3918.
(48) Jin, X.; Fiore, A.; Boersma, K. F.; Smedt, I. D.; Valin, L. Inferring Changes in Summertime Surface Ozone-NOx-VOC Chemistry over U.S. Urban Areas from Two Decades of Satellite and Ground-Based Observations. *Environ. Sci. Technol.* **2020**, *54* (11), 6518−6529.
(49) Perdigones, B. C.; Lee, S.; Cohen, R. C.; Park, J.-H.; Min, K.-E. Two Decades of Changes in Summertime Ozone Production in California's South Coast Air Basin. *Environ. Sci. Technol.* **2022**, *56*, 10586.
(50) Murphy, J. G.; Day, D. A.; Cleary, P. A.; Wooldridge, P. J.; Millet, D. B.; Goldstein, A. H.; Cohen, R. C. The Weekend Effect within and Downwind of Sacramento – Part 1: Observations of Ozone, Nitrogen Oxides, and VOC Reactivity. *Atmospheric Chem. Phys.* **2007**, *7* (20), 5327−5339.
(51) Ott, W. R. A Physical Explanation of the Lognormality of Pollutant Concentrations. *J. Air Waste Manag. Assoc.* **1990**, *40* (10), 1378−1383.
(52) Seltzer, K. M.; Murphy, B. N.; Pennington, E. A.; Allen, C.; Talgo, K.; Pye, H. O. T. Volatile Chemical Product Enhancements to Criteria Pollutants in the United States. *Environ. Sci. Technol.* **2022**, *56* (11), 6905−6913.
(53) Zhao, Y.; Li, Y.; Li, Y.; Kumar, A.; Ying, Q.; Kleeman, M. J. Reducing Southern California Ozone Concentrations in the Year 2050 under a Low Carbon Energy Scenario. *Atmos. Environ.* **2024**, *320*, No. 120315.
(54) Wu, S.; Alaimo, C.; Green, P.; Young, T.; Zhao, Y.; Liu, S.; Kuwayama, T.; Kleeman, M. J. Source Apportionment of Volatile Organic Compounds (VOCs) in South Coast Air Basin (SoCAB) During RECAP-CA, In preparation.
(55) Jiang, Z.; Shi, H.; Zhao, B.; Gu, Y.; Zhu, Y.; Miyazaki, K.; Lu, X.; Zhang, Y.; Bowman, K. W.; Sekiya, T.; Liou, K.-N. Modeling the Impact of COVID-19 on Air Quality in Southern California: Implications for Future Control Policies. *Atmospheric Chem. Phys.* **2021**, *21* (11), 8693−8708.

https://doi.org/10.1021/acsestair.4c00026
ACS EST Air 2024, 1, 536−546